Available online at www.sciencedirect.com
SCIENCE DIRECT®
Bioelectrochemistry 63 (2004) 327–332
Bioelectrochemistry
www.elsevier.com/locate/bioelechem

# Osmotically induced membrane tension facilitates the triggering of living cell electropermeabilization ☆

C. Barrau, J. Teissié, B. Gabriel *

*Institut de Pharmacologie et de Biologie Structurale-CNRS, UMR5089, 205 route de Narbonne, Toulouse cedex 4, F-31077 France*

Received 23 June 2003; received in revised form 13 November 2003; accepted 17 November 2003

**Abstract**

Very little is known about the molecular mechanisms supporting living cell membrane electropermeabilization. This concept is based on the local membrane permeability induced by cell exposure to brief and intense external electric field pulses. During the electric field application, an electro-induced membrane electric potential difference is created that is locally associated with the dielectric properties of the plasma membrane. When the new membrane electric potential difference locally reaches a critical value, a local alteration of the membrane structure is induced and leads to reversible permeabilization. In our study, we attempted to determine whether mechanical tension could modulate the triggering of membrane electropermeabilization. Change in lateral tension of Chinese Hamster Ovary cell membrane has been osmotically induced. Cell electropermeabilization was performed in the minute time range after the osmotic stress, i.e., before the regulatory volume decrease being activated by the cell. Living cell electropermeabilization was analyzed on cell population using flow cytometry. We observed that electropermeabilization triggering was significantly facilitated when the lateral membrane tension was increased. The main conclusion is that the critical value of transmembrane potential needed to trigger membrane electropermeabilization, is smaller when the membrane is under lateral mechanical constraint. This supports the hypothesis that both mechanical and electrical constraints play a key role in transient membrane destabilization.


*Keywords:* Electropermeabilization; Electroporation; Transmembrane potential; Membrane tension; Osmotic stress

## 1. Introduction

Cell electropermeabilization is the transient permeabilization of the plasma membrane by means of short (micro- to millisecond) and intense (hundred V/cm) external electric field pulses. More recently electropermeabilization of cell membranes has strongly attracted consideration for application in biology, biotechnology and medicine [1]. Despite its widespread use, the physical and structural bases of cell membrane destabilization remain unclear. During the electric field application (electropulsation) on the cell, an electro-induced membrane electric potential difference ($\Delta\Psi_i$) is created which is locally associated with the dielectric properties of the plasma membrane. Using a physical model based on a thin, weakly conductive shell (the membrane, conductivity $\lambda_m$) full of an internal conductive medium (the cytoplasm, conductivity $\lambda_i$), and immersed in an external conductive medium (conductivity $\lambda_e$), solution of the Laplace's differential equation gives $\Delta\Psi_i$ as:

$$\Delta\Psi_i(M,E,t) = -fg(\lambda)rE\cos[\theta(M)](1-\mathrm{e}^{-t/\tau_m}) \quad (1)$$

where $M$ is the point on the cell we are considering, $t$ is the time after electropulsation is turned on, $f$ is a factor depending on the cell geometry (for a sphere, $f=1.5$), $r$ is the radius of the pulsed cell, $E$ is the electric field strength, and $\theta(M)$ is the angle between the direction of the field and the normal of the cell surface in $M$. $g(\lambda)$ is related to the different conductivities as [2]:

$$g(\lambda) = 2\lambda_e\,[2\lambda_m+\lambda_i+(\lambda_m-\lambda_i)(r-d/r)^3 - 3\lambda_m(r-d/r)]/[(2\lambda_e+\lambda_m)(2\lambda_m+\lambda_i) + 2(r-d/r)^3(\lambda_i-\lambda_m)(\lambda_m-\lambda_e)] \quad (2)$$

☆ Presented at the 17th BEB symposium in Florence (Italy), 2003.

* Corresponding author. Tel.: +33-5611-758-10; fax: +33-5611-759-97.
*E-mail address:* bruno.gabriel@ipbs.fr (B. Gabriel).

1567-5394/$ - see front matter © 2004 Elsevier B.V. All rights reserved.
doi:10.1016/j.bioelechem.2003.11.009

where $d$ is the thickness of the membrane. $\tau_m$ is the characteristic time constant of the membrane charging and can be written as [3]:

$$\tau_m = rC_m(2\lambda_e + \lambda_i)/(2\lambda_e\lambda_i) \quad (3)$$

where $C_m$ ($=0.5-1.0$ μF/cm$^2$) is the specific membrane capacitance. $\tau_m$ is calculated to be in the microsecond time range. If the plasma membrane is considered to be a pure spherical dielectric ($\lambda_m = 0$), we obtain $g(\lambda) = 1$. In these conditions and when the steady state is reached ($t \gg \tau_m$) as for millisecond pulses, Eq. (1) simplifies to:

$$\Delta\Psi_i(M,E) = -1.5rE\cos[\theta(M)] \quad (4)$$

When living cells are electropulsed, $\Delta\Psi_i$ adds to the resting one $\Delta\Psi_0$. When the new membrane electric potential difference $|\Delta\Psi_0 \pm \Delta\Psi_i|$ locally reaches a critical value ($\Delta\Psi_c$) (nowadays estimated between 0.25 and 0.6 V for living cells [4–7]), a local alteration of the membrane structure leads to membrane permeabilization. The biological relevance of Eq. (1) (geometry and kinetics) has been experimentally demonstrated on single cells by use of potential sensitive dyes [8,9] and environment-dependent dyes [7, 10]. Electropermeabilization is a local event on the cell surface and the region affected by the electric pulse is linearly related to the reciprocal of the field intensity ($1/E$) [11,12].

Recently, the notion that local changes in membrane electric fields might strongly control basic and ubiquitous membrane processes was developed with the "molecular electroporation" concept. The membrane pore formation mediated by exogenous proteins (annexin V and antibacterial peptides) was described using the "molecular electroporation" concept [13–15]. In this case, local electropermeabilization of the lipid bilayer by the electrostatic field due to charged molecules that bind to the membrane surface, supports this new mechanistic concept. Such concept was also proposed to describe membrane fusion involved in exocytosis in adrenal chromaffin cells [16]. Due to the asymmetrical distribution of negatively charged phospholipids in the membrane, the close apposition of the two membranes at the site of exocytosis induces the electrostatic field strength to reach values sufficiently high to cause local membrane electropermeabilization which can then trigger the fusion of the two membranes. Transient breakdown of the membrane at the junction site in synaptic transmission was also proposed to be triggered by electrostatic interaction energy between oppositely charged interfaces (negatively charged cytosolic leaflet of the membrane, and positively charged residues of the synaptic SNARE complex of the vesicle) [17,18]. In this case, calcium ions are supposed to be implicated in the lipid bilayer breakdown mechanism. The electrostatic interaction energy in concert with calcium ions may drive discrete micellizations of the apposed membranes which may generate the transient "fusion pore" [18]. More recently, both mechanical (membrane tension) and electrical (membrane electric potential difference) local constraints were showed to play a key role in exocytosis-associated membrane fusion [19]. In the present study, we attempted to determine whether mechanical tension could modulate the triggering of membrane electropermeabilization. Change in lateral tension of Chinese Hamster Ovary cell membrane has been osmotically induced. We observed that the critical value of transmembrane electrical potential difference ($\Delta\Psi_c$) needed to trigger membrane electropermeabilization, was smaller when the membrane was under mechanical constraint. This supports the hypothesis that both mechanical and electrical constraints could play a key role in transient membrane destabilization.

## 2. Experimental

### 2.1. CHO cell culture

CHO cells (WTT clone) adapted for suspension culture were used to avoid trypsin treatment when cells were collected. They were grown in suspension in a 8% fetal calf serum complemented Eagle's minimum medium MEM 0111 (Eurobio, Les Ulis, France; $\pi = 330 \pm 4$ mOs/kg) as previously described [20].

### 2.2. Reagents

Propidium Iodide (PI, MW 668.4) was purchased from Sigma (St Louis, USA). bis-(1,3-Dibutylbarbituric acid)-trimethine oxonol ($DiBaC_4(3)$) was obtained from Molecular Probes (Eugene, OR). Isoosmotic ($\pi = 280 \pm 3.3$ mOs/kg, Osmomat 030 cryoscopic osmometer; Gonotec, Berlin, Germany) pulsing buffer (PB) was 250 mM sucrose (Sigma), 1 mM $MgCl_2$, and 10 mM HEPES (Sigma) (pH 7.4). Hypoosmotic pulsing buffer (PBH) ($\pi = 102 \pm 2$ mOs/kg) was 75 mM sucrose, 1 mM $MgCl_2$, and 10 mM HEPES (pH 7.4). Conductivities were 1.215 and 1.375 mS/cm at 21 °C (HI 8820 N conductivity meter; Hanna instruments, Lingolsheim, France) for PBI and PBH, respectively.

### 2.3. Osmotic stress and associated transient cell size increase

CHO cells ($10^6$) were collected by centrifugation for 7 min at $100 \times g$ and resuspended in 120 μl of 100 μM PI containing PBH (or PBI for control). Due to the culture medium-containing pellet death volume, the final osmotic pressure was $\pi = 120 \pm 4.4$ mOs/kg ($282 \pm 2$ mOs/kg for control). Cell diameter changes associated with the osmotic stress were determined using a video-microscope (direct measurement of cell diameters on the monitor) and by flow cytometry (FACScan, Becton Dickinson, San Jose, CA) (average forward light scattering, FSC). In this case, average

cell diameter measurement was achieved using Flow Cytometer Size Calibration Kit (Molecular Probes).

### 2.4. Determination of transmembrane electrical potential difference

$DiBaC_4(3)$ was a potentiometric slow-response probe, which accumulates in the cytoplasm of depolarized cells in a Nernst equilibrium-dependent way. Using nanomolar concentrations of dye (50–500 nM), for which the activity of oxonol ions is considered to be proportional to the fluorescence emission intensity, the Nernst equation can be then resolved using the ratio of fluorescence intensities measured outside ($F_{out}$) and inside ($F_{in}$) the cell:

$$\Delta\Psi = \Psi_{in} - \Psi_{out} = -(RT/zF)\ln(F_{in}/F_{out}) \quad (5)$$

where $R$ is the gas constant (=8.31 J/mol K), $z$ is the charge number of oxonol monovalent anions (=−1), and $F$ is Faraday's constant (=96,500 C/mol). Determination of transmembrane electrical potential difference values ($\Delta\Psi$) was adapted from what was previously described for suspended cells using flow cytometry [21].

### 2.5. Cell electropermeabilization

Cell electropermeabilization was performed in the minute time range after the osmotic stress. CHO cells ($10^6$) were collected by centrifugation for 7 min at 100 × $g$ and resuspended in 120 μl of 100 μM PI containing appropriate pulsing buffer. Cell suspension (100 μl) was placed between two stainless-steel parallel electrodes seated on the bottom of a dish. Inter-electrode width was 0.5 cm. Electropermeabilization was performed at room temperature using a CNRS electropulser (Jouan, St Herblain, France) which delivered DC square-wave pulses. Pulse parameters were monitored through a 15-MHz oscilloscope (Enertec, St Etienne, France). Cell electropermeabilization was quantified by penetration of the impermeant dye PI. Five minutes after electropulsation, cells were resuspended in 1 ml of buffer and analyzed by flow cytometry, gating the scatters (FSC and SSC) to exclude debris. The excitation wavelength was 488 nm (argon laser) and the fluorescence of intracellular PI was collected in FL-2 channel (bandpass 585 ± 42 nm). A minimum of $5 \times 10^3$ events were acquired in list mode and analyzed with Cellquest software (Becton Dickinson).

### 2.6. Data processing

All experiments were repeated at least three times on different days. Results are presented as mean and standard error on the mean. On the permeabilization curves, a two-parameter sigmoid was fitted as previously described [22]:

$$y(E,T) = a(T)/(1 + e^{[(E_{50}(T)-E)/b]}) \quad (6)$$

where $y(E,T)$ is the fraction of electropermeabilized cells (%), $a(T)$ is the maximal fraction of electropermeabilized cells (%), $E_{50}(T)$ is the electric field strength corresponding to electropermeabilization of 50% of the cells, and $b$ is the slope of the sigmoid curve. All fits were obtained by least-squares linear and nonlinear regression using EasyPlot 4.0.1 (Spiral Software, MIT). Correlation coefficients were systematically higher than 0.94. Paired $t$-test were achieved using Prism 2.01 software (GraphPad Software).

## 3. Results and discussion

### 3.1. Transient cell swelling and regulatory volume decrease

In isoosmotic medium (280 ± 3.3 mOs/kg), suspended CHO cells exhibited a spherical shape and had a gaussian-like size distribution with a mean diameter of 13.8 ± 1.60 μm. No change in cell size was observed with time (Fig. 1). In hypoosmotic medium (120 ± 4.4 mOsm/kg), CHO cells remained spherical with gaussian-like size distribution but swelled significantly in the minute time range. The mean cell diameter increased to 14.7 ± 2 μm, 2 min after the osmotic stress, and then decrease to 12.75 ± 1.90 μm,

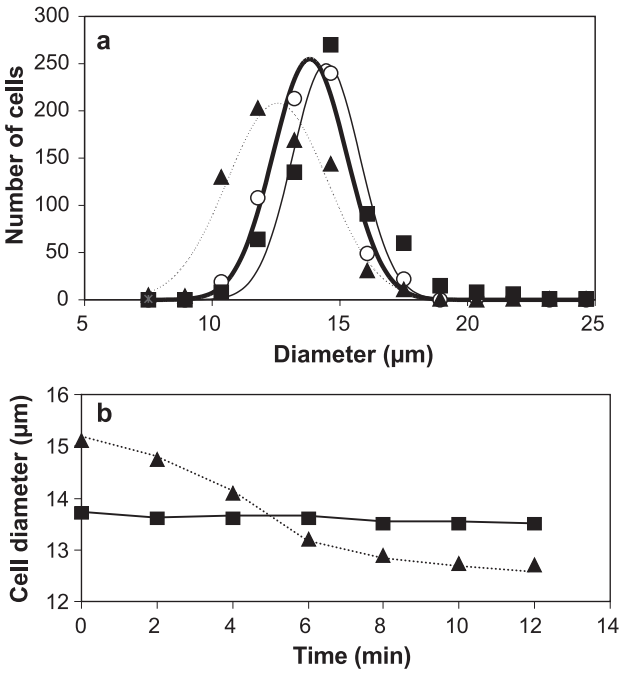


Fig. 1. Hypoosmotically induced transient CHO cell swelling. (a) Cell size statistical distribution before (PBI, 280 mosM/kg) (○), 2 min (■), and 10 min (▲) after the hypoosmotic stress (PBH, 200 mosM/kg). Mean cell diameters were 13.8 ± 1.6 μm (sampling, $n$=655 cells), 14.7 ± 2.0 μm (sampling, $n$=659 cells), and 12.75 ± 1.90 μm (sampling, $n$=701 cells), respectively. Cell diameters were measured under a video-microscope. Experimental data were fitted by normal law. (b) Cell size changes with time after the osmotic stress (▲) in comparison with native cells (isoosmotic buffer) (■). Mean cell diameters were estimated by flow cytometry (average FSC value).

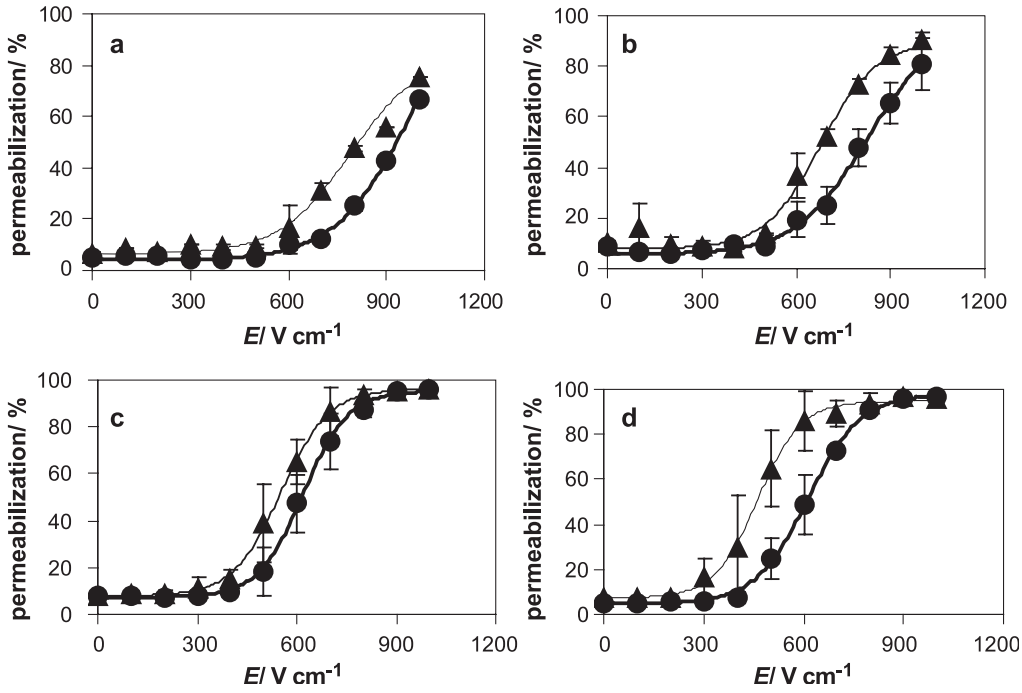


Fig. 2. Effect of osmotic stress on the CHO cell electropermeabilization. Cell suspension received one single electric pulse of 0.5 ms (a), 1 ms (b), 5 ms (c), and 10 ms (d) in 100 μM PI-containing PBH (▲) or PBI (●). Electropermeabilization was monitored 10 min after pulsation by flow cytometry (FL-2 channel (bandpass 585 ± 42 nm)), 5000 events. Data were analyzed with Cellquest software (Becton Dickinson) and fitted using two-parameter sigmoids (see Eq. (6)).

10 min after the osmotic stress (Fig. 1a). Maximum in cell size increase was reached less than 1 min after the osmotic stress. Then, the cells shrunk toward a mean cell diameter smaller than the native one (Fig. 1b). Hypoosmotic stress caused initial cell swelling due to the uptake of water driven by the imposed osmotic gradient (hypotonic swelling). This led to a significant cell size increase in the seconds following the osmotic stress. Then activated volume recovery pathways (regulatory volume decrease) took place. This CHO cell-controlled phenomenon lasted for 10–12 min. It is based on the activation of specific ion transport pathways [23].

### 3.2. Cell electropermeabilization

Cell electropermeabilization was performed 2 min after the osmotic stress, i.e., before the regulatory volume decrease being significantly activated by the cell. In our conditions, no increased uptake of propidium iodide was observed in osmotically stressed cell before the electrical treatment. Fig. 2 shows the electropermeabilization plots obtained for CHO cell suspension in iso- and hypoosmotic media. Electrical conditions were one pulse of variable duration (0.5–10 ms) and electric field strength. In the two osmotic conditions, electro-induced PI incorporation

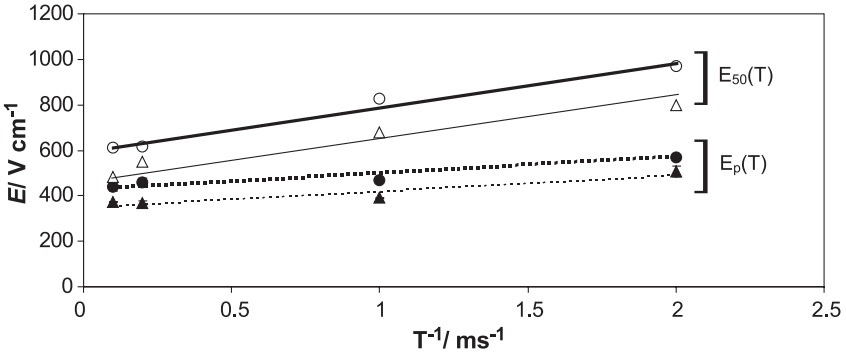


Fig. 3. Effect of the duration of the pulse on cell electropermeabilization. $E_p(T)$ and $E_{50}(T)$ values were estimated from the permeabilization curves reported in Fig. 2. CHO cells were pulsed by one single pulse with variable duration in 100 μM containing pulsing buffer. Effect of the duration on the pulse on $E_p(T)$ in PBI (●, crit = 433 ± 23 V/cm) and in PBH (▲, crit = 357 ± 14 V/cm ), and on $E_{50}(T)$ in PBI (○, crit = 596 ± 36 V/cm) and in PBH (△, crit = 489 ± 43 crit = 489 ± 43 V/cm ) are reported. Correlation coefficients of the straight line were all higher than 0.97. Extrapolation to infinite duration gave the critical values (crit) for $E_p(T)$ and $E_{50}(T)$.

Table 1
Influence of the osmotic pressure on Eq. (4) associated parameters for CHO cell suspension

| Osmotic pressure (mOs $kg^{-1}$) | Average cell radius (μm)[a] | Critical $E_{50}$ (V $cm^{-1}$)[b] | Resting TMP difference (mV) |
|---|---|---|---|
| 282 ± 2 | 13.8 ± 1.6 | 596 ± 36 | − 61 ± 1.5 |
| 120 ± 4.4 | 14.7 ± 2.0 | 489 ± 43 | − 44.5 ± 9 |

Data are mean and standard error on the mean.
[a] Cell radii were measured 2 min after cell suspension in appropriate buffer.
[b] Cells were pulsed with one single electric pulse.

into cells was only detected for electric strengths higher than an apparent threshold value ($E_p(T)$), which depended on the pulse duration. Above this threshold value, any increase in the electric field strength led to an increase of the fraction of electropermeabilized cells. A plateau value was reached for the longest pulse durations (5 and 10 ms). However, a shift to lower electric field strengths was systematically observed when the cells were electropulsed under hypoosmotic conditions while the sigmoid shape of the curve was not change. Influence of pulse duration on the $E_p(T)$ and $E_{50}(T)$ (Eq. (6)) values was analyzed. Whatever the osmotic conditions, increasing the pulse duration resulted in a decrease in $E_p(T)$ and $E_{50}(T)$ (Fig. 2). For the two osmotic conditions, a linear relationship was found between the reciprocal of pulse duration and $E_p(T)$ or $E_{50}(T)$ (Fig. 3). Extrapolation for infinite pulse duration allowed determination of critical values for $E_p(T)$ and $E_{50}(T)$. For CHO cells electropulsed in isoosmotic medium, $E_p(T)$ and $E_{50}(T)$ were equal to 433 ± 23 and 596 ± 36 V/cm, respectively. For CHO cells electropulsed in hypoosmotic medium, $E_p(T)$ and $E_{50}(T)$ were equal to 357 ± 14 and 489 ± 43 V/cm, respectively. Ratios between the two $E_p(T)$ values, and the two $E_{50}(T)$ values, which had been obtained in the two osmotic conditions, were very close (1.213 and 1.219, respectively), as expected for homothetic curves (Fig. 2). This result can be related to the global shift of the statistical cell-size distribution to higher diameters when the cell are under hypoosmotic stress (short time effects).

### 3.3. Transmembrane electrical potential (TMP) difference changes

Changes in resting transmembrane electrical potential difference value has been previously reported during CHO cells regulatory volume decrease [23]. NaCl-mediated hypoosmotic stress produced a rapid depolarization of the cell membrane. Such a rapid and transient depolarization has been also observed with cultured human fibroblasts [24]. Using the fluorescent oxonol $DiBaC_4(3)$ dye, we measured the transmembrane electrical potential differences for CHO cells under our iso- and hypoosmotic conditions (Table 1). Measurements were achieved in the minute time range after osmotic stress, as for electropermeabilization. Resting transmembrane electrical potential difference values were found to be − 61 ± 1.5 mV for cells suspended in isoosmotic medium, and − 44.5 ± 9 mV for cells suspended in hypoosmotic medium. The hypoosmotically induced cell depolarization presumably reflects the increased anion conductance observed in hypoosmotically shocked cells.

### 3.4. Critical transmembrane electrical potential difference for electropermeabilization

In our conditions, we assumed that $fg(\lambda)$ was equal to 1.5 and, that $\tau_m$ was in the microsecond time range as theoretically predicted [25]. From the critical $E_{50}$ values obtained in this study (Table 1) and using the simplified Eq. (4), we could then roughly approximate the absolute $\Delta\Psi_c$ values needed to trigger membrane electropermeabilization in iso- and hypoosmotic conditions. We found 678 ± 68 mV for native CHO cells (isoosmotic condition), and 580 ± 60 mV for hypoosmotic shocked CHO cell. These two significantly different values ($p < 0.0001$) support the hypothesis that membrane lateral tension facilitates the triggering of electropermeabilization as previously proposed for lipid model vesicles [26]. Such synergetic effect of osmotically induced membrane tension on model membrane permeabilization has been also observed for Class L amphipatic helical peptides [27]. It was concluded that the transient formation of large defect formation (membrane destabilization) was strongly enhanced by the membrane tension. However, in living cells, membrane tension was assumed to be isotropic in the membrane plane and strongly dependent on cytoskeleton and glycocalix interactions with the membrane core [28]. Previous work using the cell-attached patch-clamp configuration showed that membrane tension effect on electrically induced patched-membrane breakdown was different for short (50 μs) and long (100 ms) pulses [29]. In this work, we showed that for pulses smaller than 10 ms, the critical threshold for membrane permeabilization decreased with lateral tension suggesting that in our conditions, a large part of the mechanical stress applied on the cell reached the membrane bilayer. Our observations support the hypothesis that both mechanical and electrical constraints could play a key role in transient membrane destabilization. Such synergetic effect between these two constraints could play a major role in protein-mediated *molecular electroporation*, by limiting the effect of the protein-induced interfacial electric field to the stretched lipid-region in contact with the protein.

## References

[1] R.O. Potts, Yu.A. Chizmadzhev, Opening doors for exogenous agents, Nat. Biotechnol. 16 (1998) 135.
[2] U. Zimmermann, G. Pilwat, F. Riemann, Dielectric breakdown of cell membranes, Biophys. J. 14 (1974) 881–899.
[3] K. Kinosita Jr., T.Y. Tsong, Voltage-induced pore formation and hemolysis of human erythrocytes, Biochim. Biophys. Acta 471 (1977) 227–242.
[4] T.C. Tomov, I.C. Tsoneva, Changes in the surface charge of cells induced by electrical pulses, Bioelectrochem. Bioenerg. 22 (1989) 127–133.

[5] P. Marszalek, D.S. Liu, T.Y. Tsong, Schwan equation and transmembrane potential induced by alternating electric field, Biophys. J. 58 (1990) 1053–1058.
[6] J. Teissié, M.P. Rols, An experimental evaluation of the critical potential difference inducing cell membrane electropermeabilization, Biophys. J. 65 (1993) 409–413.
[7] B. Gabriel, J. Teissié, Direct observation in the millisecond time range of fluorescent molecule asymmetrical interaction with the electropermeabilized cell membrane, Biophys. J. 73 (1997) 2630–2637.
[8] D. Gross, L.M. Loew, W.W. Webb, Optical imaging of cell membrane potential changes induced by applied electric fields, Biophys. J. 50 (1986) 339–348.
[9] K. Kinosita Jr., I. Ashikawa, N. Saita, H. Yoshimura, H. Itoh, K. Ikegami, A. Ikegami, Electroporation of cell membrane visualized under a pulsed-laser fluorescence microscope, Biophys. J. 53 (1988) 1015–1019.
[10] K. Schwister, D. Deutike, Formation and properties of aqueous leaks induced in human erythrocytes by electrical breakdown, Biochim. Biophys. Acta 816 (1985) 332–348.
[11] B. Gabriel, J. Teissié, Mammalian cell electropermeabilization as revealed by millisecond imaging of fluorescent changes of ethidium bromide in interaction with the membrane, Bioelectrochem. Bioenerg. 47 (1998) 113–118.
[12] B. Gabriel, J. Teissié, Time courses of mammalian cell electropermeabilization observed by millisecond imaging of membrane property change during the pulse, Biophys. J. 76 (1999) 2158–2165.
[13] A. Karshikoff, R. Bareness, A. Burger, H.D. Lux, A. Cavalie, R. Huber, Annexin V membrane interaction: an electrostatic potential study, Eur. Biophys. J. 20 (1992) 337–344.
[14] E. Neumann, P.M. Siemens, K. Toensing, Electroporative fast pore-flickering of the annexin V–lipid surface complex, a novel gating concept for ion transport, Biophys. Chem. 86 (2000) 203–220.
[15] M. Miteva, M. Andersson, A. Karshikoff, G. Otting, Molecular electroporation: a unifying concept for the description of membrane pore formation by antibacterial peptides, exemplified with NK-lysin, FEBS Lett. 462 (1999) 155–158.
[16] K. Rosenheck, Evaluation of the electrostatic field strength at the site of exocytosis in adrenal chromaffin cells, Biophys. J. 75 (1998) 1237–1243.
[17] R.B. Sutton, D. Fasshauer, R. Jahn, A.T. Brunger, Crystal structure of a SNARE complex involved in synaptic exocytosis at 2.4 Å resolution, Nature 395 (1998) 347–353.
[18] M. Montal, Electrostatic attraction at the core of membrane fusion, FEBS Lett. 447 (1999) 129–130.
[19] C. Ramos, J. Teissié, Tension–voltage relationship in membrane fusion and its implication in exocytosis, FEBS Lett. 465 (2000) 141–144.
[20] B. Gabriel, J. Teissié, Generation of reactive-oxygen species induced by electropermeabilization of Chinese hamster ovary cells and their consequence on cell viability, Eur. J. Biochem. 223 (1994) 25–33.
[21] Z. Krasznai, T. Marian, L. Balkay, M. Emri, L. Tron, Flow cytometric determination of absolute membrane potential of cells, J. Photochem. Photobiol. 28 (1995) 93–99.
[22] G. Pucihar, T. Kotnik, M. Kanduser, D. Miklavcic, The influence of medium conductivity on electropermeabilization and survival of cells in vitro, Bioelectrochemistry 54 (2001) 107–115.
[23] B. Sarkadi, L. Attisano, S. Grinstein, M. Buchwald, A. Rothstein, Volume regulation of Chinese hamster ovary cells in anisoosmotic media, Biochim. Biophys. Acta 774 (1984) 159–168.
[24] V. Dall'Asta, R. Gatti, G. Orlandini, P.A. Rossi, B.M. Rotoli, R. Sala, O. Bussolati, G.C. Gazzola, Membrane potential changes visualized in complete growth media through confocal laser scanning microscopy of bis-Oxonol-loaded cells, Exp. Cell. Res. 231 (1997) 260–268.
[25] T. Kotnik, F. Bobanonic, D. Miklavcic, Sensitivity of transmembrane voltage induced by applied electric field—A theoretical analysis, Bioelectrochem. Bioenerg. 43 (1997) 285–291.
[26] D. Needham, R.M. Hochmuth, Electro-mechanical permeabilization of lipid vesicles. Role of membrane tension and compressibility, Biophys. J. 55 (1989) 1001–1009.
[27] I.V. Polozov, G.M. Anantharamaiah, J.P. Segrest, R.M. Epand, Osmotically induced membrane tension modulates membrane permeabilization by Class L amphipatic helical peptides: nucleation model of defect formation, Biophys. J. 81 (2001) 949–959.
[28] M.P. Sheetz, J. Dai, Modulation of membrane dynamics and cell mobility by membrane tension, Trends Cell Biol. 6 (1996) 85–89.
[29] J. Akinlaja, F. Sachs, The breakdown of cell membrane by electrical and mechanical stress, Biophys. J. 75 (1998) 247–254.